Journal of Geochemical Exploration 163 (2016) 10–18

Contents lists available at ScienceDirect

Journal of Geochemical Exploration

journal homepage: www.elsevier.com/locate/gexplo

Depth influence on the distribution of chemical elements and saturation index of mineral phases in twins maar lakes: The case of the Monticchio lakes (southern Italy)

Michele Paternoster [a,b,*], Giovanni Mongelli [a], Antonio Caracausi [b], Rocco Favara [b]

[a] Department of Sciences, University of Basilicata, Campus di Macchia Romana, Viale dell'Ateneo Lucano 10, Potenza, Italy
[b] Istituto Nazionale di Geofisica e Vulcanologia (INGV), Sezione di Palermo, Via Ugo La Malfa 153, Palermo, Italy

ARTICLE INFO

Article history:
Received 17 April 2015
Revised 23 December 2015
Accepted 3 January 2016
Available online 5 January 2016

Keywords:
Lake water
Meromictic lake
Chemical elements and saturation index
Depth control
Mineral phases

ABSTRACT

In this paper we provide a systematic geochemical study of the Monticchio maar lakes, on the Mt. Vulture volcano, southern Italy, to understand the processes affecting the distribution of chemical elements. A high-resolution conductivity–temperature–depth profile was obtained, and water samples were collected at various depths for analyses of major and trace elements. Although the two lakes are separated by less than 200 m, they exhibit different behaviour. The Ca–Na–HCO_3 composition of "Lago Grande" water suggests that low-temperature fluids are leached from the host volcanic rocks. Na–Ca–HCO_3 in near-surface "Lago Piccolo" water is derived from the dissolution of local volcanic rocks, while the deepest water samples are bicarbonate alkaline-earth in composition and generally show an enrichment in solutes with respect to the epilimnion layer (except for SO_4^{2-} content). The hypolimnion water is principally governed by both the input of saline groundwater from the lake bottom and authigenic processes within bottom sediments. In addition, the occurrence of anoxic conditions and microbial activity is responsible for the transformation of sulphates to hydrogen sulphide, and for the precipitation of Fe sulphide phases. Both processes cause a change in the chemical composition of saline groundwater as it moves upwards. Overall, the water chemistry of the Monticchio lakes is principally affected by: i) the input of CO_2-rich volcanic gas; ii) evaporative processes that deplete near-surface water in some elements; and iii) the occurrence of chemical, physical and biological conditions causing the transformation of molecular complexes and consequently promoting mineral precipitation.

1. Introduction

There have been increasing concerns about water quality in lakes (Kingsford, 2011), and a growing interest in understanding their physico-chemical features. The evaluation of processes governing the chemical stratification of lake water is, therefore, a powerful tool for lake management practices (Gal et al., 2009). Lakes support important freshwater ecosystems and biodiversity, regulate the water cycle, supply water resources, and maintain ecological balance (Rubec and Hanson, 2009). The Lago Piccolo (hereafter LP) and Lago Grande (hereafter LG) lakes occupy two explosive maar craters on the Mt. Vulture volcano, southern Italy. Both the LP and LG maar craters were created by intense explosive volcanic activity when a relatively small volume of erupted magma sprayed out over a large area. The Mt. Vulture hydrogeological basin is one of the most important aquifers in southern Italy (e.g., Parisi et al., 2011a, 2011b), and is also situated on a popular tourist route because of its high scenic and ecological value. Various studies have been conducted in the lakes for paleoclimate reconstruction (Brauer et al., 2000), the genesis of sediments (Schettler and Albéric, 2008) and geochemical characteristics (conductivity–temperature–depth profiles, major ions, isotopic (O and H) composition and dissolved gas content, e.g. Caracausi et al., 2009, 2013b; Chiodini et al., 1997, 2000a). Water chemistry data show that although the two lakes are separated by less than 200 m, they have different dynamics: LP is a meromictic lake, whereas LG is a warm monomictic lake, which exhibits complete water turnover in winter and a subsequent new chemical stratification during the spring (Caracausi et al., 2013b). Previous studies on the isotopic composition (δD and $\delta^{18}O$) of groundwater and rainwater in the Mt. Vulture area (Caracausi et al., 2013b; Marini, 2006; Mongelli et al., 1975) indicate that LP waters deeper than 25 m fall along the local meteoric water line (LMWL, Paternoster et al., 2008), whereas LP shallow water and all LG water exhibit a linear trend, which is typical of evaporative processes as in other volcanic lakes (e.g. Varekaamp and Kreulen, 2000).

The trophic state and pollution level in lakes can mask minute compositional changes in water geochemistry. Therefore, these changes may be more efficiently recorded by the geochemical behaviour of

* Corresponding author at: Department of Sciences, University of Basilicata, Campus di Macchia Romana, Viale dell'Ateneo Lucano 10, Potenza, Italy.
E-mail address: michele.paternoster@unibas.it (M. Paternoster).

http://dx.doi.org/10.1016/j.gexplo.2016.01.001
0375-6742/

trace elements (e.g. Sugiyama et al., 2005) than solely from the distribution of major ions and the isotopic composition. In this respect, the two Mt. Vulture lakes, which share the same origin, hydrogeological basin and climate, offer a unique opportunity to evaluate how different water dynamics affect the distribution of trace elements with depth. With this in mind, we present the first large chemical dataset from the lakes that includes Li, B, Al, V, Mn, Co, Fe, Ni, Cu, Zn, As, Rb, Se, Sr, Mo, Sb, Cd, Cs, Ba and Pb, in addition to major ions. These data are used to evaluate processes that affect the distribution of chemical elements as a function of the depth through the water column of both lakes.

2. Hydrogeology of the Mt. Vulture area

Mt. Vulture is a Quaternary stratovolcano, located along the external edge of the Apennine Chain (Fig. 1) in the northeastern sector of the Basilicata region (Italy). Volcanic activity began during the middle–upper Pleistocene (0.73 M.yr. ago) and ended 0.13 M.yr. ago (Büettner et al., 2006). Recently Caracausi et al. (2013a) show that the region around Mt. Vulture is affected by an active degassing of mantle-derived fluids through a NE–SW lithospheric discontinuity (Vulture Line). Volcanics are undersaturated silica pyroclastic deposits and subordinate lava flows composed of tephritic-phonolite, phonofoidite, foidite, melilitite and carbonatites (Beccaluva et al., 2002; Giannandrea et al., 2006). The area is characterized by NW–SE, NNW–SSE and E–W oriented normal fault systems (Beneduce and Giano, 1996; Schiattarella et al., 2005) that control the evolution of the drainage system, principally oriented along NW–SE and E–W axes (Ciccacci et al., 1999). The average rainfall is 830–900 mm/yr. and the average annual temperature is 13.7–14.1 °C (AA.VV, 2006), indicating a sub-humid (C2B′2sb′3) climate according to the classification scheme proposed by Thornthwaite and Mather (1957).

The Mt. Vulture aquifer core is mainly composed of pyroclastic and subordinate lava flow layers of different permeabilities, which give rise to distinct aquifer layers. The principal hydrogeological complexes are therefore volcanic products, with high-medium permeability values. The structural hydraulic parameters and anisotropy features of the aquifer are the major factors that control groundwater flow pathways (Parisi et al., 2011a). A recent hydraulic and hydrogeochemical study (Parisi et al., 2011a) enabled a detailed characterization of the aquifer. This study found that:

i). Groundwater geochemistry is heterogeneous between different sectors, and there are two hydrogeochemical water types, reflecting different low-temperature water–rock interactions. The first water type has bicarbonate alkaline and alkaline-earth composition with a relatively low salinity (hereafter LS), whereas the second water type has bicarbonate-sulphate alkaline composition with higher salinity (hereafter HS).

ii). Three main sectors can be distinguished within the Mt. Vulture hydrogeological system. The first W–NW sector, which constitutes the main recharge area, has an isotopic signature similar to rainwater. The second and third sectors represent the main S–SE and N–NE discharge areas.

Lake volumes are 3.98×10^6 m^3 and 3.25×10^6 m^3 for LG and LP, respectively. Surface areas are 4.3×10^5 m^2 and 1.7×10^5 m^2 for LG and LP, respectively. The two lakes are connected by a 200 m long channel, through which LP water flows toward LG (Caracausi et al., 2013b). The Monticchio lakes are situated at 660 m a.s.l. and the estimated mean recharge altitude is about 925 m a.s.l. (Caracausi et al., 2013b).

3. Sampling and methods

Water samples were collected in June 2010 in both Monticchio lakes. Water was collected vertically along a water column from the surface down to the bottom at the deepest point of each lake. A 2 L clear polycarbonate sampler was used to collect deep lake water. Physical and chemical parameters were obtained using a high-resolution probe (Ageotec IM71) equipped with a pH sensor. The temperature probe has an accuracy of 0.01 °C and resolution of 0.001 °C; the accuracy values of the electrical conductivity (EC) and pH sensors are 0.005 mS cm^{-1} and 0.01 units, respectively. The spatial acquisition step of temperature, EC and pH data was 1 m (Table 1). All water samples were filtered through a 0.45 μm MF-Millipore membrane

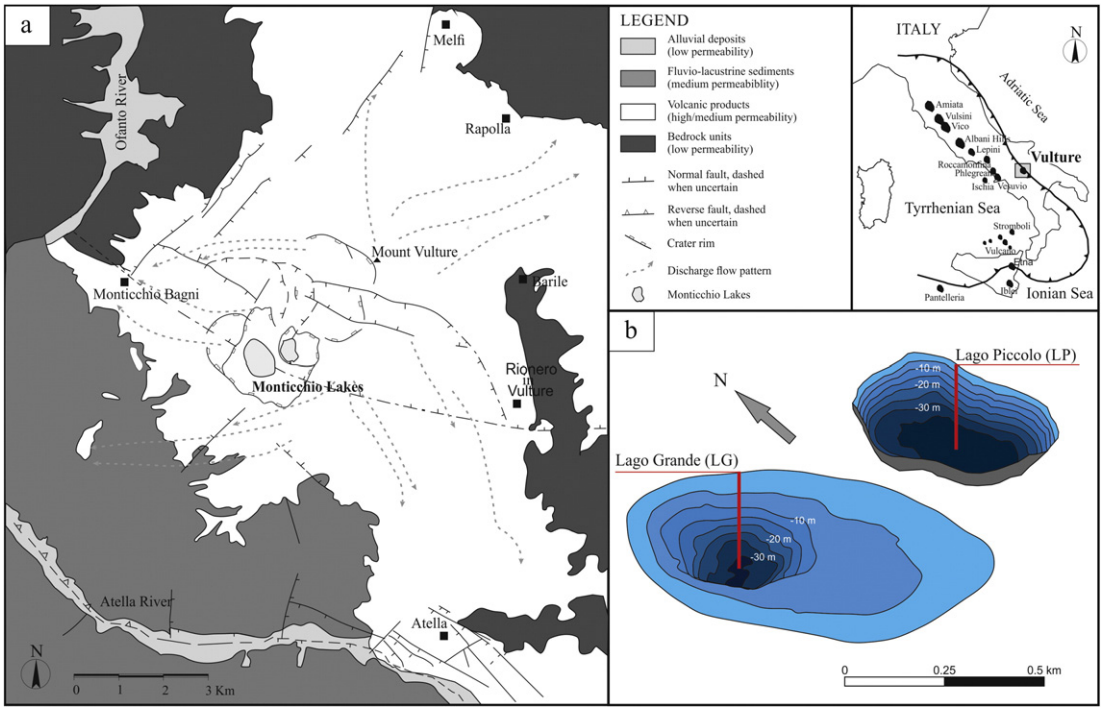

Fig. 1. (a) Simplified geological map of the Mt. Vulture volcano (modified from Giannandrea et al., 2006). (b) Bathymetric map of the Monticchio lakes showing the sampling points. The discharge flow water lines from Parisi et al. (2011a).

Table 1
In situ measurements of chemical and physical parameters of the Monticchio lake water.

	Lago grande (LG)			Lago piccolo (LP)		
Depth	T	EC	pH	T	EC	pH
Meter	°C	mS/cm		°C	mS/cm	
−0.3	19.41	0.418	8.35	19.45	0.362	8.09
−1	19.25	0.418	8.26	19.25	0.360	8.10
−2	17.63	0.410	7.50	18.92	0.358	8.05
−3	16.29	0.399	7.25	17.64	0.347	8.12
−4	12.98	0.385	7.09	15.53	0.334	7.85
−5	9.85	0.377	6.92	11.91	0.308	7.52
−6	8.13	0.361	6.87	9.83	0.293	7.69
−7	7.36	0.354	6.83	8.53	0.284	7.48
−8	7.05	0.349	6.82	7.81	0.280	7.27
−9	6.91	0.348	6.80	7.32	0.277	7.06
−10	6.73	0.346	6.77	6.91	0.276	6.91
−11	6.61	0.344	6.74	6.70	0.275	6.81
−12	6.57	0.343	6.73	6.54	0.276	6.71
−13	6.53	0.343	6.72	6.45	0.279	6.64
−14	6.50	0.344	6.70	6.57	0.300	6.40
−15	6.47	0.344	6.65	6.91	0.573	6.06
−16	6.45	0.345	6.63	7.13	0.620	6.04
−17	6.44	0.346	6.60	7.28	0.635	6.04
−18	6.43	0.346	6.58	7.36	0.642	6.04
−19	6.43	0.347	6.56	7.44	0.651	6.04
−20	6.42	0.348	6.52	7.52	0.660	6.04
−21	6.41	0.349	6.52	7.60	0.668	6.04
−22	6.41	0.349	6.49	7.68	0.676	6.04
−23	6.41	0.350	6.48	7.74	0.684	6.04
−24	6.40	0.351	6.47	7.81	0.691	6.04
−25	6.40	0.351	6.46	7.86	0.697	6.04
−26	6.40	0.351	6.45	7.92	0.706	6.04
−27	6.40	0.351	6.44	7.95	0.710	6.04
−28	6.40	0.352	6.43	8.00	0.713	6.04
−29	6.40	0.353	6.43	8.08	0.731	6.04
−30	6.40	0.353	6.43	8.19	0.757	6.04
−31	6.40	0.353	6.42	8.31	0.793	6.05
−32	6.40	0.353	6.41	8.41	0.828	6.05
−33	6.40	0.354	6.39	8.53	0.876	6.05
−34	6.40	0.354	6.39	8.67	0.952	6.06
−35	6.40	0.355	6.40	8.77	1.020	6.07
−36	–	–	–	8.88	1.117	6.08
−37	–	–	–	8.95	1.184	6.09

Note: T = temperature; EC = electrical conductivity;–is for not measured. See text for further details.

in the field, and then stored in high-density polyethylene bottles (50 and 100 mL). The bottles were filled to the top with water, capped without leaving any headspace, stored in a refrigerated container (ca. 4 °C) during transportation to the laboratory, and then kept cool until analysis. At each sampling point, one water sample (for cation analyses) was collected and acidified in the field with ultrapure HNO_3; a second unacidified sample was collected for anion analysis, and a third sample was acidified (with ultrapure HCl) for trace element analysis. Major ion concentrations were determined by ion chromatography using a Dionex AS14A Ion Pac for anions (F^-, Cl^-, NO_3^- and SO_4^{2-}) and Dionex CS-12 A Ion Pac for cations (Na^+, K^+, Mg^{2+} and Ca^{2+}). Experimental accuracy is better than ±3%, except for the deepest LP water sample where the presence of organic acids could not to be excluded. Alkalinity was determined in the field by titration with HCl (0.1 M). The NH_4^+ content was obtained by Nessler colorimetric method (Jeong et al., 2013 and reference therein), in which potassium, mercury, and iodine react with to create a yellow-brownish coloured compound. A spectrophotometer (Shimatzu UV–VIS), with an analytical error below 0.1 ppm, was used. Dissolved trace elements were determined using high-precision inductively coupled plasma-quadrupole mass spectroscopy (ICP-MS). All trace element determinations were performed with the external standard calibration method, using NIST and SLRS standard reference materials for calibration. The precision of the analytical results was estimated by running triplicate analyses every ten samples. Uncertainty of measurements is ≤12% for all the trace analytes. Silica was determined spectrophotometrically using the b-silicomolybdenum blue method, at k = 650 nm. All laboratory analysis was performed at the "Istituto Nazionale di Geofisica e Vulcanologia, Sezione di Palermo".

4. Results

4.1. Water chemistry

pH, temperature (T) and electric conductivity (EC) data are shown in Fig. 2 and reported in Table 1, while the chemical composition of water samples in Tables 2a and 2b. Relative concentrations of dissolved major ions are compared with the composition of local groundwater and local rainwater in Fig. 3. The distributions of selected chemical constituents with depth are plotted in Figs. 4 and 5.

4.1.1. Lago Piccolo

In LP, T decreases sharply from 19.45 °C in the shallowest sample to 6.57 °C at a depth of about 14 m (Fig. 2). Below this depth, temperature increases slightly, suggesting that heat flows upward from the bottom (Caracausi et al., 2013b and references therein). EC decreases from 0.362 mS cm^{-1} in the shallowest sample to the 0.300 mS cm^{-1} at a depth of about 14 m. Between 14 m and 15 m, EC increases abruptly (fluctuating in the 0.300–0.573 mS cm^{-1} range), and below 16 m, EC increases sharply to the maximum value of 1.184 mS cm^{-1} at 37 m.

The T profile from June 2010 shows three distinct thermal regions: an epilimnion extending from surface to a depth of about 14 m, an intermediate layer with a thickness of about 2 m (from 14 m to 16 m) and a hypolimnion extending below 16 m depth. This stratification is similar to the findings of Caracausi et al. (2013b), and suggests that meromixis is associated with a salinity increase in the deepest layers. Finally, pH is 8.09 in the shallowest sample, 6.06 at a depth of about 15 m, and constant below this (Fig. 2).

T, EC and pH profiles suggest that a significant change in the water chemistry occurs in the LP water column. This change is shown in ternary plots of Ca^{2+}, Mg^{2+}, Na^+, and HCO_3^-, SO_4^{2-} and Cl^- (Fig. 3). In the epilimnion layer, samples LP3, LP8 and LP12 have a Na–Ca–HCO_3 composition, whereas the deepest water samples are bicarbonate alkaline-earth in composition. Overall, concentrations of major ions increase with depth (Fig. 4), except for SO_4^{2-} and F^-. Similarly, minor and trace elements are lower in the epilimnion than in the deepest layers and an abrupt increase in ammonia and all trace and minor element concentrations is observed at the interface between water and bottom sediments. The Fe contents are very high in the deepest water samples and are in the range of values of other volcanic lakes (e.g., Momoun, Nyos; Kusakabe et al., 1989; Aguilera et al., 2000; Teutsch et al., 2009). A few trace elements (such as Mo, Cu, Zn, and Pb) show higher values in shallowest water than deep ones (Fig. 5).

4.1.2. Lago Grande

In LG, T decreases abruptly from 19.41 °C at 0.3 m to 6.73 °C at 10 m, below which it is roughly constant. Similarly, EC shows an abrupt decrease from the surface (0.418 mS cm^{-1}) to 10 m (0.346 mS cm^{-1}), below which it tends to slightly increase. pH decreases toward the bottom (Table 1, Fig. 2) and the higher pH in LG surface water relative to LP likely reflects the higher dissolved CO_2 uptake rates by primary producers.

The ternary Ca^{2+}, Mg^{2+}, Na^+, and HCO_3^-, SO_4^{2-} and Cl^- plots (Fig. 3) show that LG water has an homogeneous composition close to that of LS groundwater in the region. The shallowest sample, collected at a depth of 3 m from the surface, is slightly depleted in Ca^{2+} and HCO_3^-. For other major elements, however, changes with the depth are either minor or negligible (Fig. 4). NO_3^- generally has very low concentrations throughout the lake (<0.5 mg L^{-1}), and in some cases it is not

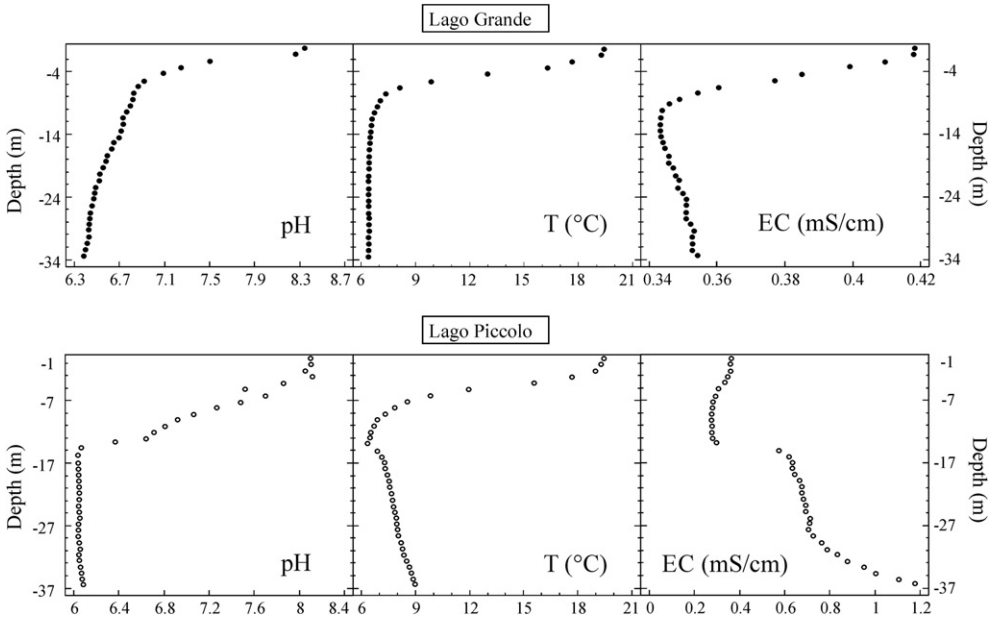

Fig. 2. pH, temperature (T) and electrical conductivity (EC) values along vertical profiles of the Monticchio Lakes.

detectable. However, NO_3^- does increase up to 7.64 mg L^{-1} at the interface between water and bottom sediments, at a depth of 35 m. Fe, Mn, Sr and Ba have a noticeable depth-controlled distribution, and increase in concentration from below 15 m depth, while the other trace elements don't change significantly with the depth (Fig. 5).

Table 2a
Chemical composition of the LP water.

		Error	Lago Piccolo (LP)							
Depth	Metre		−3	−8	−12	−18	−25	−28	−32	−37
		(%)								
Ca^{2+}	mg L^{-1}		24.3	24.7	26.5	41.3	43.8	43.4	45.5	48.3
K^+	mg L^{-1}		19.3	18.9	19.3	21.8	23.3	23.1	24.2	25.1
Mg^{2+}	mg L^{-1}		6.4	6.4	6.6	10.1	10.5	10.6	10.8	11.2
Na^+	mg L^{-1}		30.1	29.8	30.5	33.1	32.4	35.9	34.8	36.7
Si	mg L^{-1}		7.1	9.5	8.9	39	43	43	44	49
Fe	mg L^{-1}	4.7	0.006	0.007	0.011	107	125	122	132	259
HCO_3^-	mg L^{-1}		174	177	183	455	525	534	604	750
F^-	mg L^{-1}		0.9	0.9	1.0	0.6	0.7	0.7	0.6	0.6
Cl^-	mg L^{-1}		19.3	19.2	19.2	21.2	20.7	20.6	21.1	21.3
SO_4^{2-}	mg L^{-1}		8.1	8.2	8.1	0.7	0.3	0.2	0.4	0.6
NO_3^-	mg L^{-1}		b.d.l.	b.d.l.	0.28	0.16	b.d.l.	b.d.l.	b.d.l.	b.d.l.
NH_4^+	mg L^{-1}		b.d.l.	b.d.l.	b.d.l.	b.d.l.	b.d.l.	b.d.l.	b.d.l.	37.2
Li	μg L^{-1}	3.3	5.47	5.68	7.18	6.72	6.48	6.68	4.70	4.94
B	μg L^{-1}	−0.6	51	52	66	74	73	75	57	79
Al	μg L^{-1}	10.5	2.90	2.12	3.73	3.16	4.05	4.61	4.30	10.70
V	μg L^{-1}	7.2	1.89	1.39	0.41	6.14	11.2	12.1	12.6	46.1
Mn	μg L^{-1}	3.9	4.14	1.33	6.21	1853	1845	1848	1475	2495
Co	μg L^{-1}	1.3	0.06	0.07	0.09	2.11	2.08	2.02	1.57	2.34
Ni	μg L^{-1}	−1.0	0.30	0.38	0.25	0.33	0.40	0.39	0.26	0.57
Cu	μg L^{-1}	8.5	0.44	0.57	0.68	0.12	0.03	0.04	0.06	0.08
Zn	μg L^{-1}	10.9	1.94	2.35	1.80	1.18	1.09	0.81	0.57	2.13
As	μg L^{-1}	7.8	0.69	0.61	0.39	4.27	5.85	5.57	4.15	8.31
Se	μg L^{-1}	11.9	0.03	0.05	0.04	0.08	0.10	0.10	0.10	0.29
Rb	μg L^{-1}	5.7	29	29	37	39	38	40	31	54
Sr	μg L^{-1}	4.2	287	290	374	547	562	583	469	895
Mo	μg L^{-1}	−1.8	1.52	1.46	1.80	0.22	0.12	0.17	0.10	0.29
Cd	μg L^{-1}	11.0	b.d.l.	b.d.l.	b.d.l.	b.d.l.	b.d.l.	b.d.l.	b.d.l.	b.d.l.
Sb	μg L^{-1}	4.0	0.07	0.08	0.10	0.02	b.d.l.	0.01	b.d.l.	0.05
Cs	μg L^{-1}	−4.1	0.16	0.16	0.20	0.39	0.41	0.42	0.35	0.74
Ba	μg L^{-1}	−0.9	61	64	84	329	346	356	305	575
Pb	μg L^{-1}	−1.4	0.18	0.19	0.20	0.10	0.04	0.03	0.02	0.05
Charge balance	%		−0.5	−0.8	−0.5	2.0	0.9	0.7	−1.1	6.7

Note: b.d.l. = below detection limit.

Table 2b
Chemical composition of the LG water.

Depth	Metre	Error	Lago Grande (LG)						
		(%)	−3	−10	−15	−20	−25	−30	−35
Ca^{2+}	mg L^{-1}		34.6	43.1	43.1	42.4	42.5	41.5	41.9
K^{+}	mg L^{-1}		18.4	18.7	18.5	18.6	18.9	18.7	18.6
Mg^{2+}	mg L^{-1}		10.3	10.2	10.6	10.6	10.5	10.6	10.3
Na^{+}	mg L^{-1}		31.1	31	31.7	31.1	31.3	31.2	31
Si	mg L^{-1}		2.1	2.4	2.3	2.6	2.7	2.7	2.7
Fe	mg L^{-1}		0.003	0.003	0.003	0.036	0.077	0.096	0.103
HCO_3^-	mg L^{-1}		189	223	235	226	232	232	232
F^-	mg L^{-1}		0.7	0.8	0.8	0.8	0.7	0.8	0.8
Cl^-	mg L^{-1}		25.2	25	25	25.1	24.9	25.1	25.3
SO_4^{2-}	mg L^{-1}		17.3	17.8	17.9	17.3	16.7	16.8	17.1
NO_3^-	mg L^{-1}		b.d.l.	0.16	0.47	b.d.l.	b.d.l.	0.18	7.64
NH_4^+	mg L^{-1}		b.d.l.	b.d.l.	b.d.l.	b.d.l.	b.d.l.	b.d.l.	b.d.l.
Li	μg L^{-1}	3.3	2.89	2.90	2.90	2.99	2.92	3.00	2.96
B	μg L^{-1}	−0.6	57	55	56	57	56	57	56
Al	μg L^{-1}	10.5	2.82	1.24	1.27	1.36	2.28	1.73	1.70
V	μg L^{-1}	7.2	1.33	0.95	0.82	0.83	0.85	0.83	0.86
Mn	μg L^{-1}	3.9	2.46	3.5	44	1666	2254	2413	2398
Co	μg L^{-1}	1.3	0.13	0.14	0.13	0.14	0.15	0.15	0.15
Ni	μg L^{-1}	−1.0	0.30	0.32	0.35	0.37	0.42	0.37	0.38
Cu	μg L^{-1}	8.5	0.20	0.10	0.06	0.10	0.05	0.10	0.02
Zn	μg L^{-1}	10.9	0.40	0.35	0.26	0.35	0.36	0.26	0.38
As	μg L^{-1}	7.8	1.19	1.30	1.22	1.01	1.11	1.14	1.07
Se	μg L^{-1}	11.9	0.05	0.04	0.02	0.04	0.04	0.03	0.03
Rb	μg L^{-1}	5.7	32	32	32	33	33	34	33
Sr	μg L^{-1}	4.2	449	460	489	505	497	509	503
Mo	μg L^{-1}	−1.8	0.87	0.64	0.58	0.61	0.60	0.58	0.60
Cd	μg L^{-1}	11.0	b.d.l.	b.d.l.	b.d.l.	b.d.l.	b.d.l.	b.d.l.	b.d.l.
Sb	μg L^{-1}	4.0	0.09	0.06	0.05	0.07	0.07	0.07	0.08
Cs	μg L^{-1}	−4.1	0.14	0.15	0.15	0.16	0.16	0.16	0.16
Ba	μg L^{-1}	−0.9	86	94	106	129	143	146	147
Pb	μg L^{-1}	−1.4	0.05	0.06	0.05	0.06	0.05	0.03	0.03
Charge balance	%		1.1	0.2	−0.4	0.4	0.1	−0.2	−0.9

Note: b.d.l. = below detection limit.

4.2. Lake classification

The lake classification system developed by Varekamp et al. (2000) was applied to the Monticchio lakes to obtain information on the lake water category type and the features of water–rock interactions. The graph of pH vs. $Cl^- + SO_4^{2-}$ (Armienta et al., 2008; Varekamp et al., 2000) shown in Fig. 6 indicates that based on their pH values, the Monticchio lakes are classified as maar lakes. Generally, the acidity in volcanic lakes is a result of gaseous inputs from CO_2 (from deep decarbonation reactions or the oxidation of organic matter) and SO_2, and strong acids such as HCl and HF. CO_2 is the most abundant dissolved gas in Monticchio lake water (Caracausi et al., 2009, 2013b, 2015), lowering the pH and increasing leaching from the host rocks. Subsequent hydrolysis reactions consume H^+, increasing both the pH of the solution and the concentration of bicarbonate and cations. The cations released by the rocks neutralize the acidity of the water.

4.3. Water saturation state

Available analytical data enable an evaluation of the saturation state with respect to relevant mineral phases; i.e., carbonates, phyllosilicates, silicates and Fe oxi-hydroxides. The saturation index values (SI = log IAP/KS, IAP: ion activity product, KS: solubility product constant) were calculated using the equilibrium geochemical speciation/mass transfer model PHREEQC v. 2.16.04 (Parkhurst and Appelo, 1999) with the speciation model wateq. database.

In LP water, SI values are stratified with depth, moving from epilimnion to hypolimnion layer (Fig. 7). The epilimnion water are undersaturated with respect to the primary phases of volcanic rocks, with SI values decreasing with depth. Among carbonate species, calcite, dolomite and magnesite share the same trend, becoming undersaturated between the epilimnion and hypolimnion, although calcite and dolomite tend to be slightly saturated in the shallowest water strata (LP3). Conversely, siderite and rhodochrosite are undersaturated in the epilimnion, below which they tend to be saturated–oversaturated in the deepest strata. SI values indicate that Fe oxy-hydroxides are oversaturated at all depths. All phyllosilicate minerals share a similar distribution. In the epilimnion strata, water are oversaturated, except for illite, with SI values that increase initially but then decrease. This change is probably due to the precipitation rate of phyllosilicate minerals that increase with basic or near neutral pH values (Köhler et al., 2003). Deep water is undersaturated with respect to illite and montmorrilonite-Ca and oversaturated with respect to kaolinite and muscovite, with values that increase with depth.

For LG, speciation calculations (Fig. 8) indicate that water at all depths is undersaturated with respect to the primary phases of volcanic rocks; i.e., clinoenstatite, diopside, albite, anorthite and forsterite, as well as to phyllosicates minerals such as illite, montmorrilonite-Ca, Kaolinite and muscovite. In shallow water, kaolinite and muscovite are the only minerals which reached the saturation state, indicating that primary phases can dissolve and phyllosicates can precipitate. SI values indicate that, for carbonate phases, magnesite, calcite and dolomite share a similar distribution, being close to the saturation state in the shallowest strata and then decreasing with the depth. In contrast,

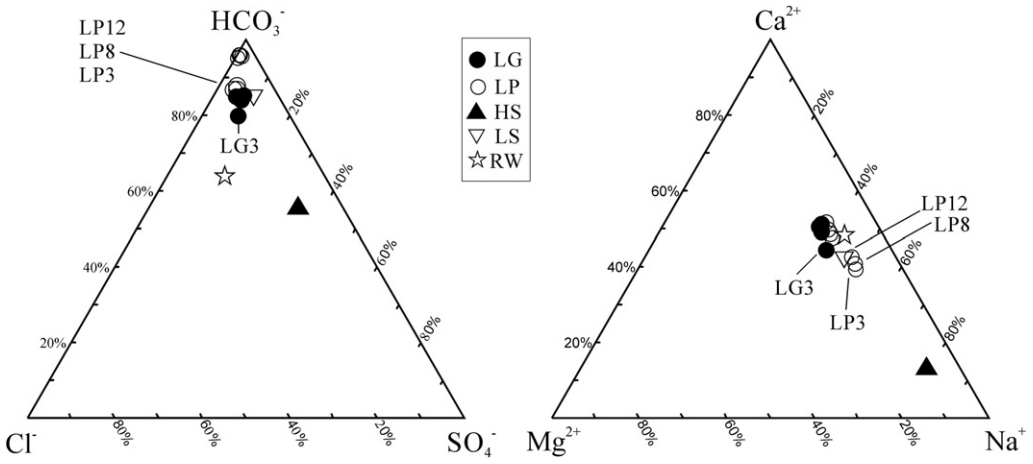

Fig. 3. Ternary diagrams of anions (HCO_3^-, SO_4^{2-} and Cl^-) and cations (Ca^{2+}, Mg^{2+}, Na^+). Relative concentrations of dissolved major ions are compared with the compositions of local groundwater (low and high salinity, LS and HS respectively) and local rainwater (RW).

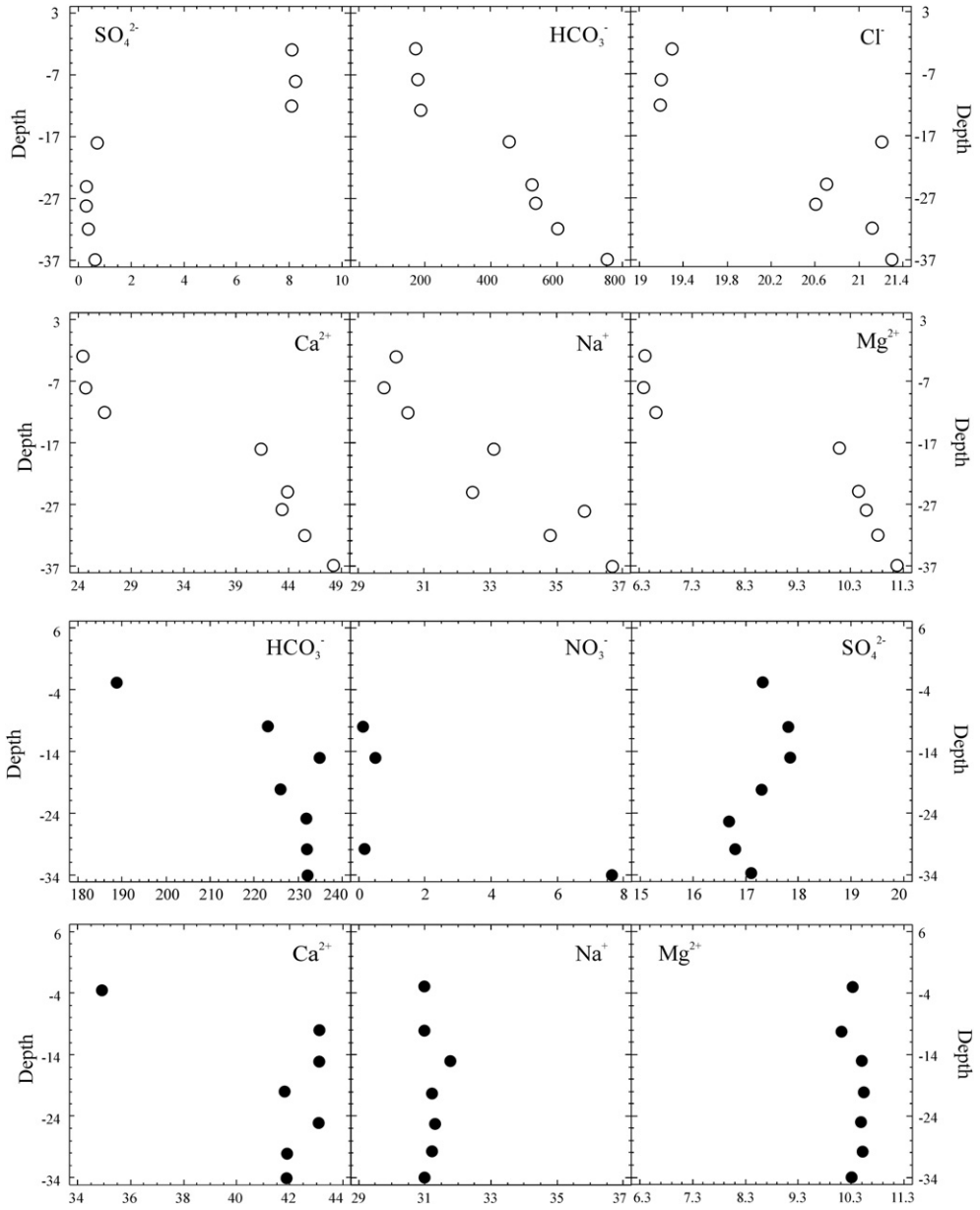

Fig. 4. Vertical profiles of the major elements in Monticchio Lake water. The values are in mg/L. Symbols as in Fig. 3.

siderite and rhodochrosite have lower values in shallow water and then only rhodochrosite tends to be close to saturation in deeper water. The latter SI values are linked to Mn concentrations, which increase rapidly with depth along the vertical profile. Similarly, SI values indicate that Fe oxi-hydroxides are oversaturated at all depths (Fig. 7).

Thermodynamic data (Figs. 7 and 8) shows that LG water overturns completely, while LP water exhibits chemical stratification. LP deep water is stagnant, with SI values that remain constant or increase slightly with depth. SI values are variable in shallower water, which is linked to both pH and precipitation-rate changes for some minerals (i.e., phyllosilicates, carbonates, Fe oxi-hydroxides).

5. Discussion

The chemical composition of volcanic lake water, not directly linked to magmatic activity, is associated with factors including: dilution/concentration processes related to rainfall and evaporation and leading to the precipitation of minerals, redox conditions, groundwater supply to the lake bottom (particularly in maars), and the composition of the host rocks. In LP, a meromictic lake with a permanent chemical stratification, the deepest water is stagnant, whereas the amount of dissolved solutes decreases alongside cyclical water circulation in the shallowest strata. Furthermore, as the contribution from meteoric water in both lakes can be neglected (Spilotro et al., 2006 and references therein), only groundwater inflow and evaporation must be considered in the lake water balance.

As in other volcanic lakes (e.g. Varekaamp and Kreulen, 2000), shallow water in LP is affected by evaporative processes, while water below 25 m depth is of meteoric origin. Since concentrations of major and trace elements in shallow water are similar to those of Mt. Vulture LS groundwater, we assume that this chemical signature is derived from the dissolution of local volcanic rocks. Hypolimnion water in the lake is anoxic, with high amounts of dissolved CO_2, mainly supplied from the bottom of the lake (Caracausi et al., 2013b, 2015). The hypolimnion layer has high salinity, and a chemical composition consistent with that of local LS groundwater (Fig. 3). This water is also stagnant and generally enriched in solutes with respect to the epilimnion layer (Figs. 5 and 6). The increase of most solutes with depth is due to the input of

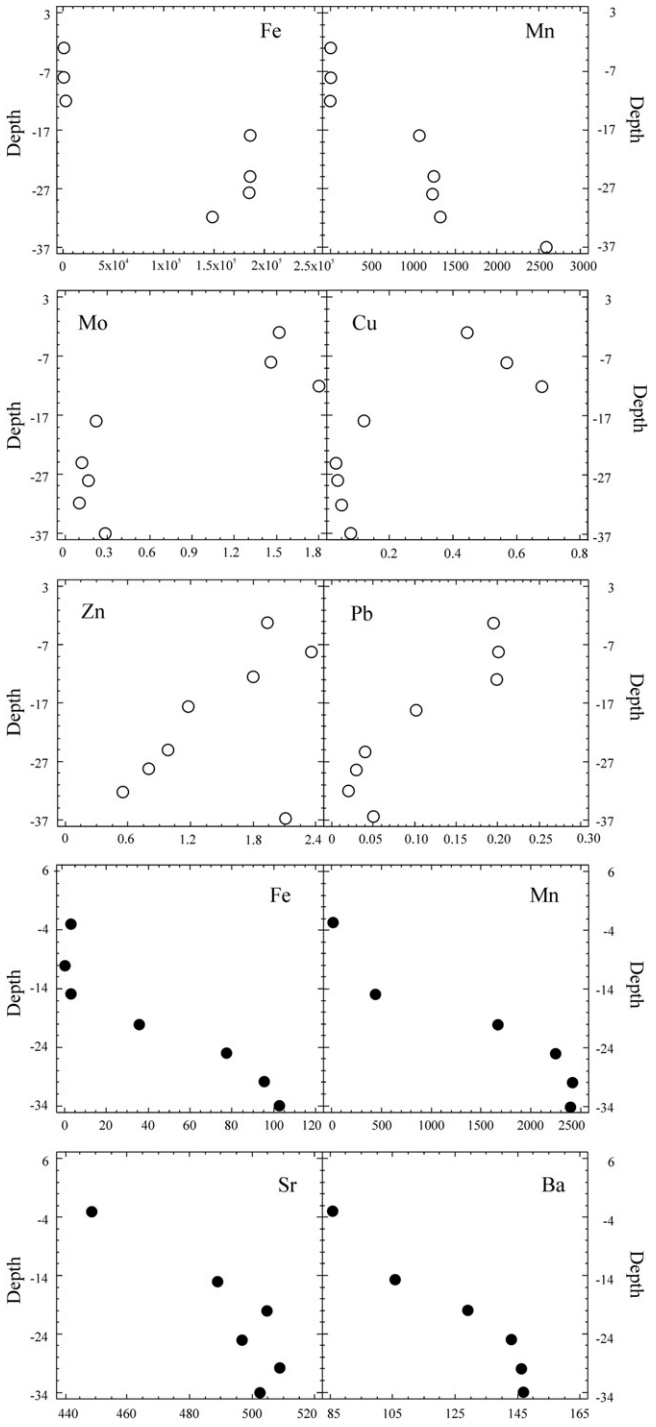

Fig. 5. Vertical profiles of a few minor and trace elements in Monticchio Lake water. The values are in μg/L. Symbols as in Fig. 3.

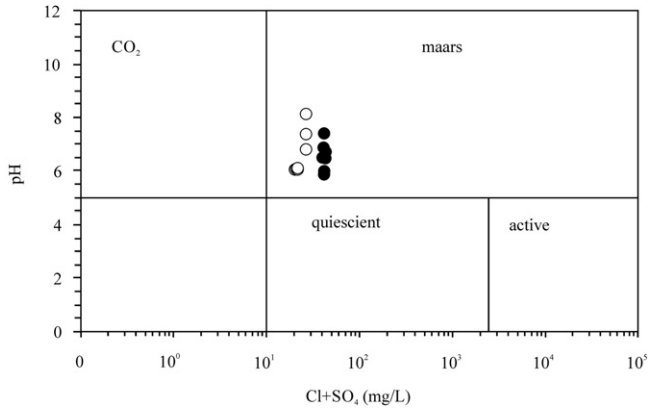

Fig. 6. pH vs. Cl + SO_4 (mg/L), modified from Varekamp et al. (2000). Fields for CO_2-dominated lakes, quiescent and active' acid crater lakes (pH < 5), and maars lakes (pH > 5) are shown. Symbols as in Fig. 3.

saline fluid from the lake bottom. Fe and Mn show a significant increase between the epilimnion and hypolimnion, and the distribution of both elements is largely controlled by redox conditions. Their oxidized forms (Mn^{4+} and Fe^{3+}) are insoluble in natural water at neutral pH, whereas their reduced forms (Mn^{2+} and Fe^{2+}) are soluble. The occurrence of anoxic conditions in the hypolimnion layer causes the observed significant increase of these elements. The highest concentrations of Fe and Mn below the oxic/anoxic interface are similar to those observed in other meromictic lakes (Balistrieri et al., 1994; Perret et al., 2000; Taillefert et al., 2000a; Tonolla et al., 1998) and are likely produced by both authigenic processes within bottom sediments (Davison, 1993) and the addition of Fe^{2+} and Mn^{2+} by saline groundwater. SO_4^{2-} decreases with the depth (Fig. 5), likely due to anaerobic conditions and microbial activity in the hypolimnion layer, as sulphur-reducing bacteria cause the transformation of sulphates to hydrogen sulphide. In Monticchio lake sediments several metal sulphide phases (including pyrite, calcopyrite and chalcocite) have been found (Schettler and Albéric, 2008), and the observed decrease in Cu, Zn, Mo and Pb with depth, suggests that these elements may co-precipitate with, or may be adsorbed on to sulphide minerals, also according to the tendency of heavier transition metal cations in lower oxidation states to preferentially join with sulphur rather than oxygen ligands (Stumm and Morgan, 1995). It is also possible that scavenging by particles either settling or resting at the sediment–water interface may decrease the concentration of some elements. The high ammonia concentration at the sediment–water interface, for example, is due to the anaerobic mineralisation of organic deposits on surface sediments.

LG is a warm monomictic lake with water isotope values (δD and $\delta^{18}O$) typical of evaporative processes. The water overturns completely during winter, confirmed by the decrease of dissolved He (Caracausi et al., 2013b), and this is followed by a new chemical stratification in spring. The concentrations of dissolved gases (CH_4, He, O_2 and Ar) vary over time and increase constantly toward the lake bottom during the spring. LG water has a Ca^{2+}–Na^{+}–HCO_3^- composition, as a result of low–temperature fluids leaching from host volcanic rocks (Parisi et al., 2011a, 2011b; Paternoster et al., 2010). The water is also characterized by high Sr concentrations (an average of 490 μg L^{-1}) and low Ca/Sr and Na/Sr ratios (84 and 63, respectively). This reflects the dissolution of carbonatite–melilitite tuff deposits in the area. Most measured elements do not show a depth-controlled distribution. Only Ca^{2+} and HCO_3^- have lower values in shallow water likely due to the precipitation of carbonate phases. High NO_3^- concentrations at the interface between water and bottom sediments are probably due to nitrification. Trace elements, Fe, Mn, Sr and Ba, increase from the shallowest to the deepest water layers. Fe and Mn are released into bottom water by reductive dissolution of Mn and Fe oxides in the sediment (Davison, 1993; Kawashima et al., 1988). Fe and Mn geochemical cycles also play a fundamental role in the behaviour of other elements, such as Sr and Ba (Sugiyama et al., 1992), which increase in the deepest water layers.

6. Conclusions

This research presents the first large chemical dataset (major, minor and trace element compositions) from the Monticchio maar lakes (Mt. Vulture volcano, southern Italy). Our results support those of previous studies (Caracausi et al., 2009, 2013b; Chiodini et al., 2000a) and indicate that, although the lakes are in close proximity, they exhibit

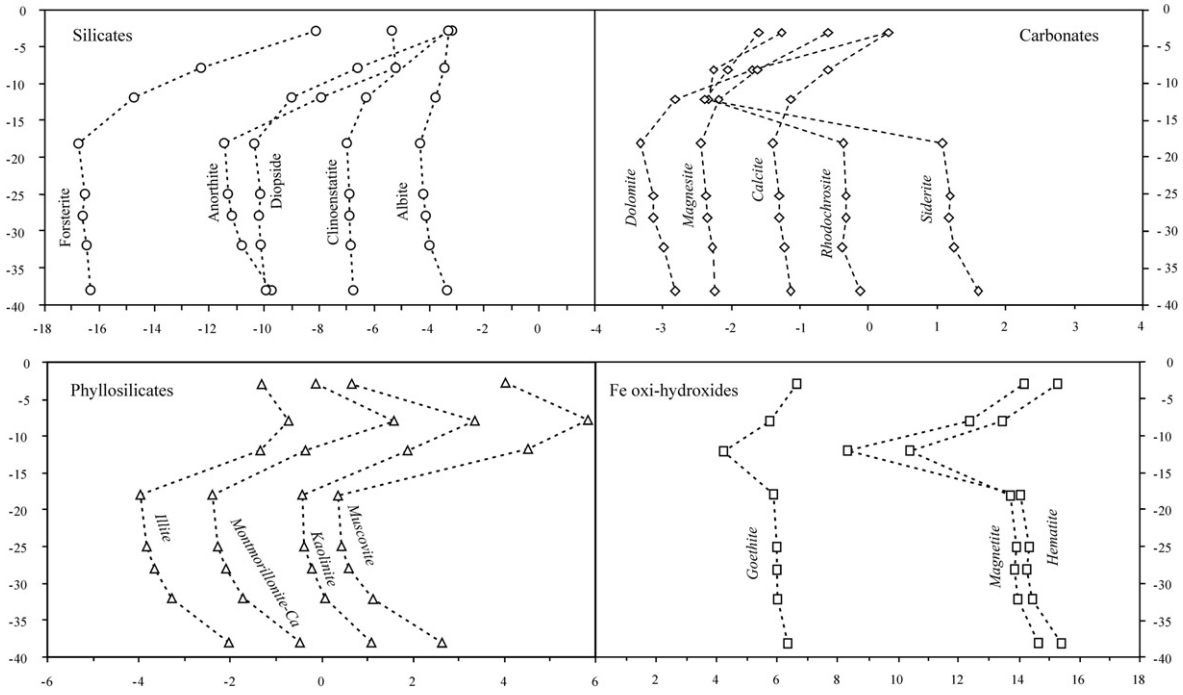

Fig. 7. Vertical profiles of the saturation index (SI) in LP water with respect to: primary phases of local volcanic rocks (silicates), phyllosilicates minerals; carbonate minerals and Fe oxi-hydroxides.

different behaviour. LG water has a Ca–Na–HCO_3 chemical composition that is close to local LS groundwater, derived from dissolution of host rocks. The lake water is fairly homogeneous, except for Ca^{2+} and HCO_3^- concentrations that have lower values in shallow layers likely due to the precipitation of carbonate phases. The chemistry of LG water is principally governed by groundwater interactions with host rocks and evaporation processes. Thermodynamic modelling of the results allows us to indicate that the LG water overturns completely while LP water exhibits chemical stratification.

LP is a meromictic lake, where shallow water (above 16 m) is affected by evaporative processes and has lower solute concentrations than deeper water layers. Shallow water exhibits homogeneous geochemical concentrations that are comparable with local LS groundwater. As for LG water, this chemical signature is derived from low-temperature fluids leaching from host volcanic rocks. The hypolimnion water are anoxic and stagnant, and have a chemical composition similar to local groundwater, but with higher salinity values. The increase of solutes with depth is due to both the input of saline fluid from the lake bottom and authigenic processes within the bottom sediments. Saline fluids from

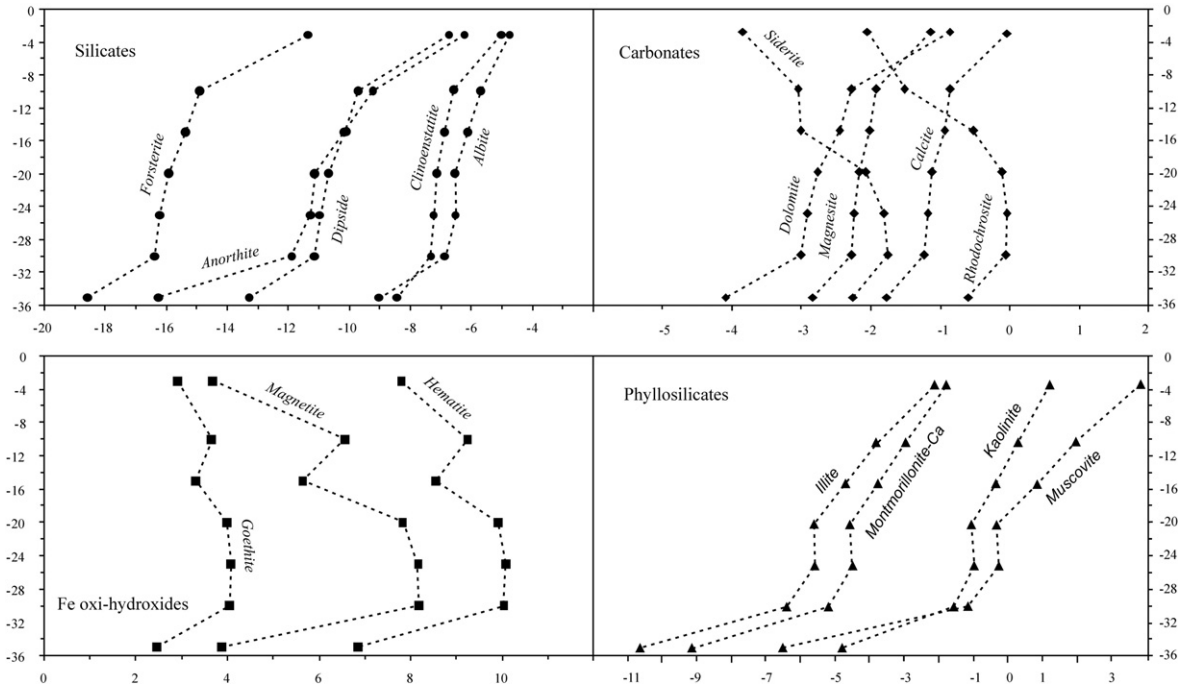

Fig. 8. Vertical profiles of the saturation index (SI) in LG water with respect to: primary phases of local volcanic rocks (silicates); phyllosilicates; carbonate minerals and Fe oxi-hydroxides.

the lake bottom could have a sulphate-bicarbonate alkaline composition, similar to that of the Mt. Vulture HS groundwater. This groundwater may subsequently modify its chemical composition to more closely reflect low salinity groundwater (Ca–Na–HCO_3) following the occurrence of anoxic conditions and microbial activity. This would cause sulphates to transform into hydrogen sulphide, and Fe sulphide phases to precipitate. Finally, the cycling of redox-sensitive elements such as Fe and Mn is found to play a fundamental role in trace element transport and concentrations.

Acknowledgements

The research was partially supported by INGV-DPC Project V5 (Research on Diffuse degassing in Italy). The authors appreciate comments by two anonymous reviewers, all of which led to significant improvements in the manuscript.

References

AA. VV. 2006. I suoli della Basilicata. Carta pedologica della Regione Basilicata in scala 1: 250.000. Regione Basilicata, Dipartimento Agricoltura, Sviluppo Rurale, Economia Montana—Ufficio Risorse Naturali in Agricoltura. http://www.basilicatanet.it/suoli/regpedologiche.htm

Aguilera, A., Chiodini, G., Cioni, R., Guidi, M., Marini, L., Raco, B., 2000. Water chemistry of lake Quilotoa (Ecuador) and assessment of natural hazards. J. Volcanol. Geotherm. Res. 97, 271–285.

Armienta, M.A., Vilaclara, G., De la Cruz-Reyna, S., Ramos, S., Ceniceros, N., Cruz, O., Arcega-Cabrera, F., 2008. Water chemistry of lakes related to active and inactive Mexican volcanoes. J. Volcanol. Geotherm. Res. 178, 249–258.

Balistrieri, L.S., Murray, J.W., Paul, B., 1994. The geochemical cycling of trace elements in a biogenic meromictic lake. Geochim. Cosmochim. Acta 58 (19), 3993–4008.

Beccaluva, L., Coltorti, M., Di Girolamo, P., Melluso, L., Dilani, L., Morra, V., Siena, E., 2002. Petrogenesis and evolution of Mt. Vulture alkaline volcanism (Southern Italy). Mineral. Petrol. 74, 277–297.

Beneduce, P., Giano, S.I., 1996. Osservazioni preliminari sull'assetto morfostrutturale dell'edificio vulcanico del M. Vulture (Basilicata) (Preliminary observations on the morpho-structural features of the M. Vulture volcanic edifice (Basilicata)). Ital. J. Quat. Sci. 9 (1), 325–330.

Brauer, A., Mingram, J., Frank, U., Günter, C., Schettler, G., Wulf, S., Zolitchka, B., Negendank, J.F.W., 2000. Abrupt environmental oscillations during the Early Weichselian recorded at Lago Grande di Monticchio, Southern Italy. Quat. Int. 73 (74), 79–90.

Büettner, A., Principe, C., Villa, I.M., Bocchini, D., 2006. ^{39}Ar–^{40}Ar geochronology of Monte Vulture. In: Principe, C. (Ed.), La Geologia del Monte Vulture. Grafiche Finiguerra, Lavello, Italy, pp. 73–86.

Caracausi, A., Nuccio, P.M., Favara, R., Nicolosi, M., Paternoster, M., 2009. Gas hazard assessment at the Monticchio crater lakes of Mt. Vulture, a volcano in southern Italy. Terra Nova 21, 83–87.

Caracausi, A., Martelli, M., Nuccio, P.M., Paternoster, M., Stuart, F.M., 2013a. Active degassing of mantle-derived fluid: a geochemical study along the Vulture line southern Apennines (Italy). J. Volcanol. Geotherm. Res. 253, 65–74.

Caracausi, A., Nicolosi, M., Nuccio, P.M., Favara, R., Paternoster, M., Rosciglione, A., 2013b. Geochemical insight into differences in the physical structures and dynamics of two adjacent maar lakes at Mt. Vulture volcano (southern Italy). Geochem. Geophys. Geosyst. 14 (5), 1606–1625.

Caracausi, A., Paternoster, M., Nuccio, P.M., 2015. Mantle CO_2 degassing at Mt. Vulture volcano (Italy): Relationship between CO_2 outgassing of volcanoes and the time of their last eruption. Earth Plan. Sci. Lett. 411, 65–74. http://dx.doi.org/10.1016/j.epsl.2014.11.049.

Chiodini, G., Cioni, R., Guidi, M., Marini, L., Principe, C., Raco, B., 1997. Water and gas chemistry of the Lake Piccolo of Monticchio (Mt. Vulture, Italy). In: Freth, S.J. (Ed.), Current Research on Volcanics Lakes, Newsletter of the IAVCEL Commission on Volcanic Lakes. 10, pp. 3–8.

Chiodini, G., Cioni, R., Guidi, M., Magro, G., Marini, L., Raco, B., 2000a. Gas chemistry of the Lake of Piccolo of Monticchio, Mt. Vulture, in December 1996. Acta Vulcanol. 12, 139–143.

Ciccacci, S., Del Gaudio, V., La Volpe., L., Sansò, P., 1999. Geomorphological features of Monte Vulture Pleistocene Volcano (Basilicata, southern Italy). Z. Geomorphol. 114 (Suppl. Bd.), 29–48.

Davison, W., 1993. Iron and manganese in lakes. Earth Sci. Rev. 34, 119–163.

Gal, G., Hipsey, M.R., Parparov, A., Wagner, U., Makler, V., Zohary, T., 2009. Implementation of ecological modeling as an effective management and investigation tool: lake Kinneret as a case study. Ecol. Model. 220, 1697–1718. http://dx.doi.org/10.1016/j.ecolmodel.2009.04.010.

Giannandrea, P., La Volpe, L., Principe, C., Schiattarella, M., 2006. Unità stratigrafiche a limiti inconformi e storia evolutiva del vulcano medio-pleistocenico di Monte Vulture (Appennino meridionale, Italia). Boll. Soc. Geol. Ital. Ital. J. Geosci. 125, 67–92.

Jeong, H., Park, J., Kim, H., 2013. Determination of NH4+ in environmental water with interfering substances using the modified Nessler method. J. Chem. 2013, 359217. http://dx.doi.org/10.1155/2013/359217.

Kawashima, M., Takamatsu, T., Koyama, M., 1988. Mechanisms of precipitation of manganese (II) in Lake Biwa, a freshwater lake. Water Res. 22, 613–618.

Kingsford, R.T., 2011. Conservation management of rivers and wetlands under climate change — a synthesis. Mar. Freshw. Res. 62, 217–222.

Köhler, S., Dufaud, F., Oelker, E.H., 2003. An experimental study of illite dissolution kinetics as a function of pH from 1.4 to 12.4 and temperature from 5 to 50 °C. Geochim. Cosmochim. Acta 67 (19), 3583–3594.

Kusakabe, M., Ohsumi, T., Aramaki, S., 1989. The lake Nyos disaster: chemical and isotopic evidence in waters and dissolved gases from three Cameroonian lake, Nyos, Monoum and Wum. J. Volcanol. Geotherm. Res. 39, 167–185.

Marini, L., 2006. Le caratteristiche isotopiche delle acque sotterranee del Monte Vulture e delle acque dei Laghi di Monticchio. In: Principe, C. (Ed.), La Geologia del Monte Vulture. Grafiche Finiguerra, Lavello, Italy, pp. 149–154.

Mongelli, F., Panichi, C., Tongiorgi, E., 1975. Studio termico ed isotopico dei crateri-laghi di Monticchio (Lucania). Arch. Oceanogr. Limnol. 18, 167–188.

Parisi, S., Paternoster, M., Kohfahl, C., Pekdeger, A., Meyer, H., Hubberten, H.W., Spilotro, G., Mongelli, G., 2011a. Groundwater recharge areas of a volcanic aquifer system inferred from hydraulic, hydrogeochemicaland stable isotope data: Mount Vulture, southern Italy. Hydrogeol. J. 19, 133–153.

Parisi, S., Paternoster, M., Perri, F., Mongelli, G., 2011b. Source and mobility of minor and trace elements in a volcanic aquifer system, Mt. Vulture (southern Italy). J. Geochem. Explor. 110, 233–244.

Parkhurst, D.K.L., Appelo, C.A.J., 1999. PHREEQC, Guide to a computer program for speciation batch –reaction, one dimensional transport, and inverse geochemical calculations. U.S. Geological Survey Water Resources Investigations Reports. 31, p. 299 (99–42559).

Paternoster, M., Liotta, M., Favara, R., 2008. Stable isotope ratios in meteoric recharge and groundwater at Mt. Vulture volcano, southern Italy. J. Hydrol. 348, 87–97. http://dx.doi.org/10.1016/j.jhydrol.2007.09.038.

Paternoster, M., Parisi, S., Caracausi, A., Favara, R., Mongelli, G., 2010. Groundwaters of Mt. Vulture volcano, southern Italy: chemistry and sulfur isotope composition of dissolved sulphate. Geochem. J. 44, 125–135.

Perret, D., Gaillard, J.F., Doninik, J., Atteia, O., 2000. The diversity of natural hydrous iron oxides. Environ. Sci. Technol. 34, 3540–3546.

Rubec, C.D.A., Hanson, A.R., 2009. Wetland mitigation and compensation: Canadian experience. Wetl. Ecol. Manag. 17, 3–14. http://dx.doi.org/10.1007/s11273-008-9078-6.

Schettler, G., Albéric, P., 2008. Laghi di Monticchio (Southern Italy, Region Basilicata): genesis of sediments—a geochemical study. J. Paleolimnol. 40 (1), 529–556. http://dx.doi.org/10.1007/s10933-007-9180-4.

Schiattarella, M., Beneduce, P., Giano, S.I., Giannandrea, P., Principe, C., 2005. Assetto strutturale ed evoluzione morfotettonica quaternaria del vulcano del Monte Vulture (Appennino Lucano). Boll. Soc. Geol. Ital. Ital. J. Geosci. 124, 543–562.

Spilotro, G., Canora, F., Caporale, F., Caputo, R., Fidelibus, M.D., Leandro, G., 2006. Idrogeologia del Monte Vulture [Hydrogeology of M. Vulture]. In: Principe, C. (Ed.), La Geologia del Monte Vulture. (The Geology of the Mount Vulture). Regione Basilicata, Potenza, Italy, pp. 123–132.

Stumm, W., Morgan, J.J., 1995. Aquatic Chemistry: Chemical Equilibria and Rates in Natural Waters. third ed. John Wiley, New York, p. 1040.

Sugiyama, M., Hori, T., Kihara, S., Matsui, M., 1992. A geochemical study on the specific distribution of barium in Lake Biwa, Japan. Geochim. Cosmochim. Acta 56, 597–605.

Sugiyama, M., Hori, T., Kihara, S., Matsui, M., 2005. Geochemical behavior of trace elements in Lake Biwa. Limnology 6 (2), 117–130.

Taillefert, M., Lienemann, C.P., Gaillard, J.F., Perret, D., 2000a. Speciation, reactivity, and cycling of Fe and Pb in a meromictic lake. Geochim. Cosmochim. Acta 64 (2), 169–183.

Teutsch, N., Schmid, M., Müller, B., Halliday, A.N., Bürgmann, H., Wehrli, B., 2009. Large iron isotope fractionation at the oxic-anoxic boundary in Lake Nyos. Earth Planet. Sci. Lett. 285, 52–60. http://dx.doi.org/10.1016/j.epsl.2009.05.044.

Thornthwaite, C.W., Mather, J.R., 1957. Instructions and tables for computing potential evapotranspiration and the water balance. Publications in Climatology vol. X. Drexel Institute of Technology, Laboratory of Climatology, Centerton, New Jersey, p. 3.

Tonolla, M., Demarta, A., Peduzzi, R., 1998. The chemistry of Lake Cadagno. Documenta dell'Istituto italiano di idrobiologia 63, pp. 11–17.

Varekaamp, J.C., Kreulen, R., 2000. The stable isotope geochemistry of volcanic lakes, with examples from Indonesia. J. Volcanol. Geotherm. Res. 97, 309–327.

Varekamp, J.C., Pasternack, G.B., Rowe, G.L., 2000. Volcanic lake systematics: II. chemical constraints. J. Volcanol. Geotherm. Res. 97, 161–179.